Simulation of the 2009, M_W = 4 Tehran earthquake using a hybrid method of modal summation and finite difference

2013 J. Geophys. Eng. 10 025007

(http://iopscience.iop.org/1742-2140/10/2/025007)

IOP Publishing Journal of Geophysics and Engineering
J. Geophys. Eng. **10** (2013) 025007 (21pp) doi:10.1088/1742-2132/10/2/025007

Simulation of the 2009, $M_w = 4$ Tehran earthquake using a hybrid method of modal summation and finite difference

Vahid Gholami[1], **Hossein Hamzehloo**[1], **Mohamad Reza Ghayamghamian**[1], **Franco Vaccari**[2,3] **and Giuliano Francesco Panza**[2,3,4]

[1] Seismology Research Center, International Institute of Earthquake Engineering and Seismology
[2] Department of Mathematics and Geosciences, University of Trieste
[3] SAND Group, The Abdus Salam International Centre for Theoretical Physics
[4] Institute of Geophysics, China Earthquake Administration, Beijing, People's Republic of China

E-mail: hhamzehloo@iiees.ac.ir

Received 1 July 2012
Accepted for publication 23 January 2013
Published 19 February 2013
Online at stacks.iop.org/JGE/10/025007

Abstract
The Greater Tehran Area is the most important city of Iran and hosts about 20% of the country's population. Despite the presence of major faults and the occurrence of historical earthquakes, the seismicity is relatively low at present. Thus, it is important to estimate the ground motion for preventive, reliable seismic hazard assessment. An earthquake with magnitude $M_w = 4$, which occurred close to Tehran, 17 October 2009, is the first local earthquake that has been recorded by the local strong ground motion network in Tehran. To simulate the ground motion caused by the earthquake a hybrid technique is used. It combines two methods: the analytical modal summation and the numerical finite difference, taking advantage of the merits of both. The modal summation is applied to simulate wave propagation from the source to the sedimentary basin and finite difference to propagate the incoming wavefield in the laterally heterogeneous part of the structural model that contains the sedimentary basin. Synthetic signals are simulated along two East–West and Southeast–Northwest profiles. Frequency, response spectra, and time domain, waveforms and peak values, parameters are computed synthetically and compared with observed records. Results show agreement between observed and simulated signals. The simulation shows local site amplification as high as 6 in the southern part of Tehran.

Keywords: Tehran, hybrid simulation, strong motion, response spectral ratio, seismic microzonation

(Some figures may appear in colour only in the online journal)

1. Introduction

Tehran, the capital city of Iran, is located in a zone with significant history of seismicity at the foot of the Alborz Mountains. The Alpine–Himalayan seismic belt is well known as one of the most seismically active areas of the world. The Iranian plateau, located in this area, has experienced several major and destructive earthquakes in the recent past. The Alborz is a narrow mountain belt, 100 km wide, which wraps around the south Caspian Sea. The mean elevation in the Alborz drops sharply from 3000 m in the inner belt to 28 m at the Caspian shoreline to the north. The topographic contrast is less pronounced to the south where the connection with the lowlands of the Central Iranian desert is progressive. Surprisingly, no crustal root has been detected below the high topography (Dehghani and Makris 1984).

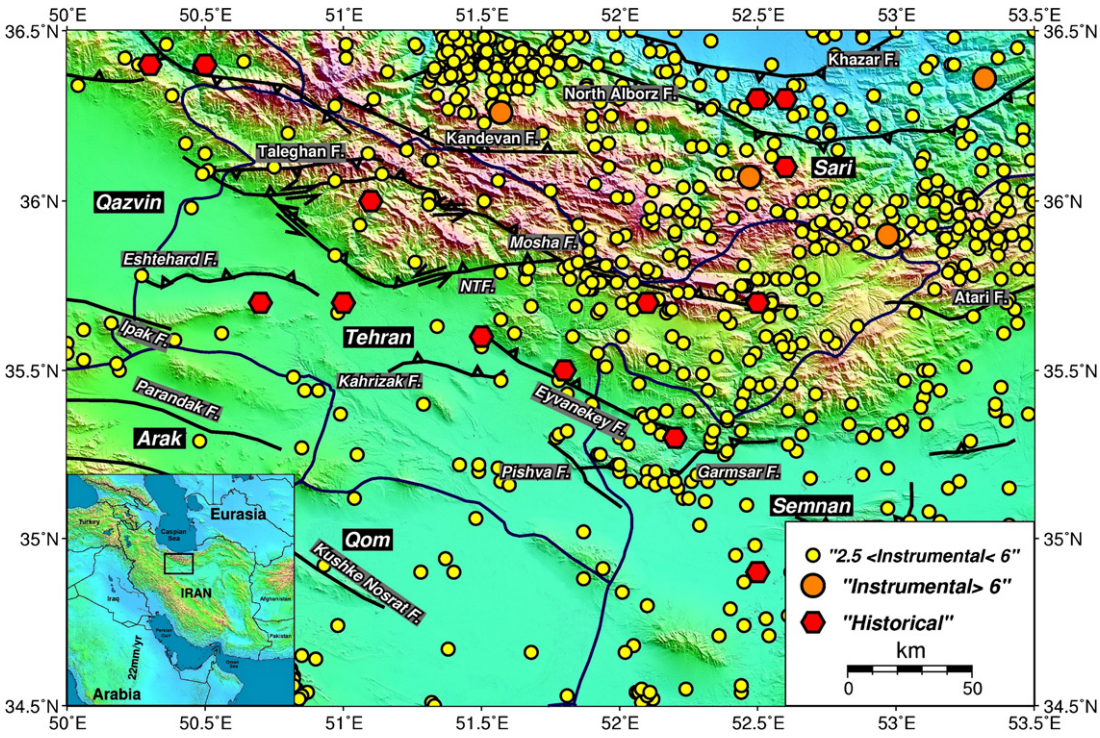

Figure 1. Distribution of instrumental and historical earthquakes on the fault map of the vicinity of Tehran. The figure clearly shows the high potential of big events inside and close to Tehran city. The reference catalogue preparing the figure is International Institute of Earthquake Engineering and Seismology, IIEES, catalogue. An overview map shows the location of the bases and implies regional tectonic setting considering Arabia and Eurasia plates.

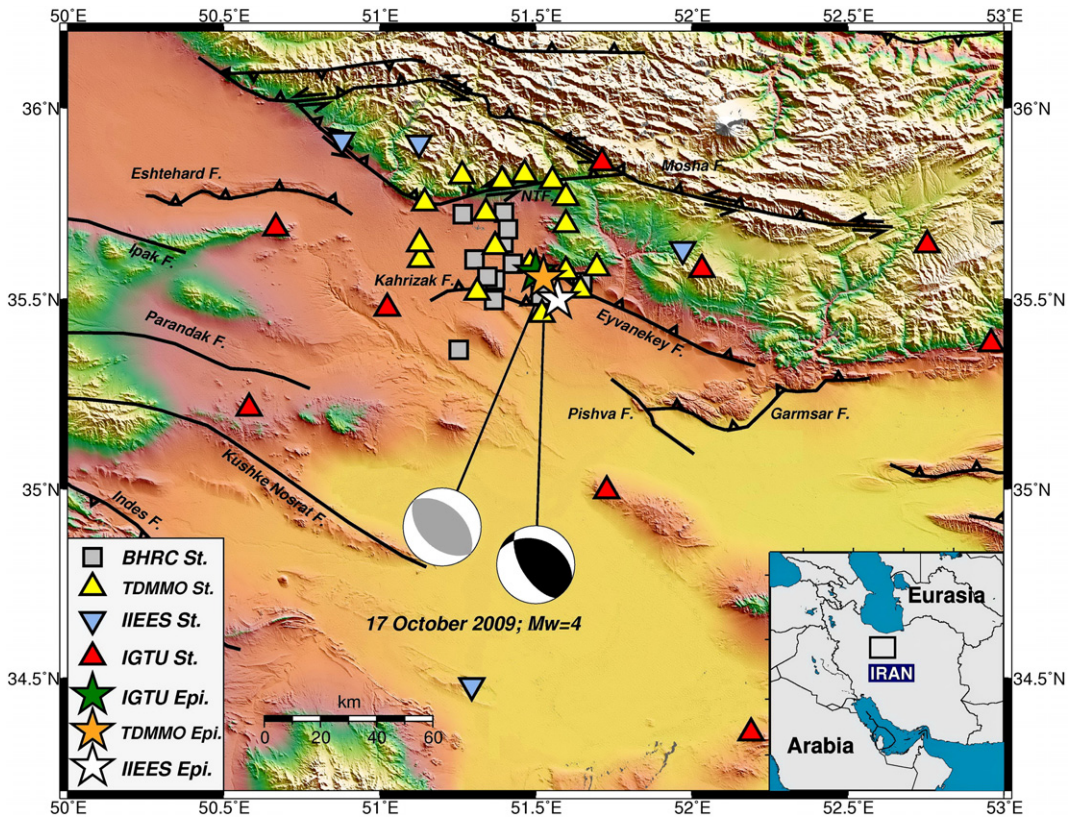

Figure 2. Distribution of IGTU (Institute of Geophysics of Tehran University), IIEES (International Institute of Earthquake Engineering and Seismology), TDMMO (Tehran Disaster Mitigation and Management Organization) and BHRC (Building and House Research Center of Iran), stations around the epicentre of 17 October 2009, $M_w = 4$ earthquake. Three different epicentres are shown by coloured stars. The two reported focal mechanisms are from Hamzehloo *et al* (2009), black, and Farahani and Zare (2011), grey. Some major faults of the region are shown and labelled.

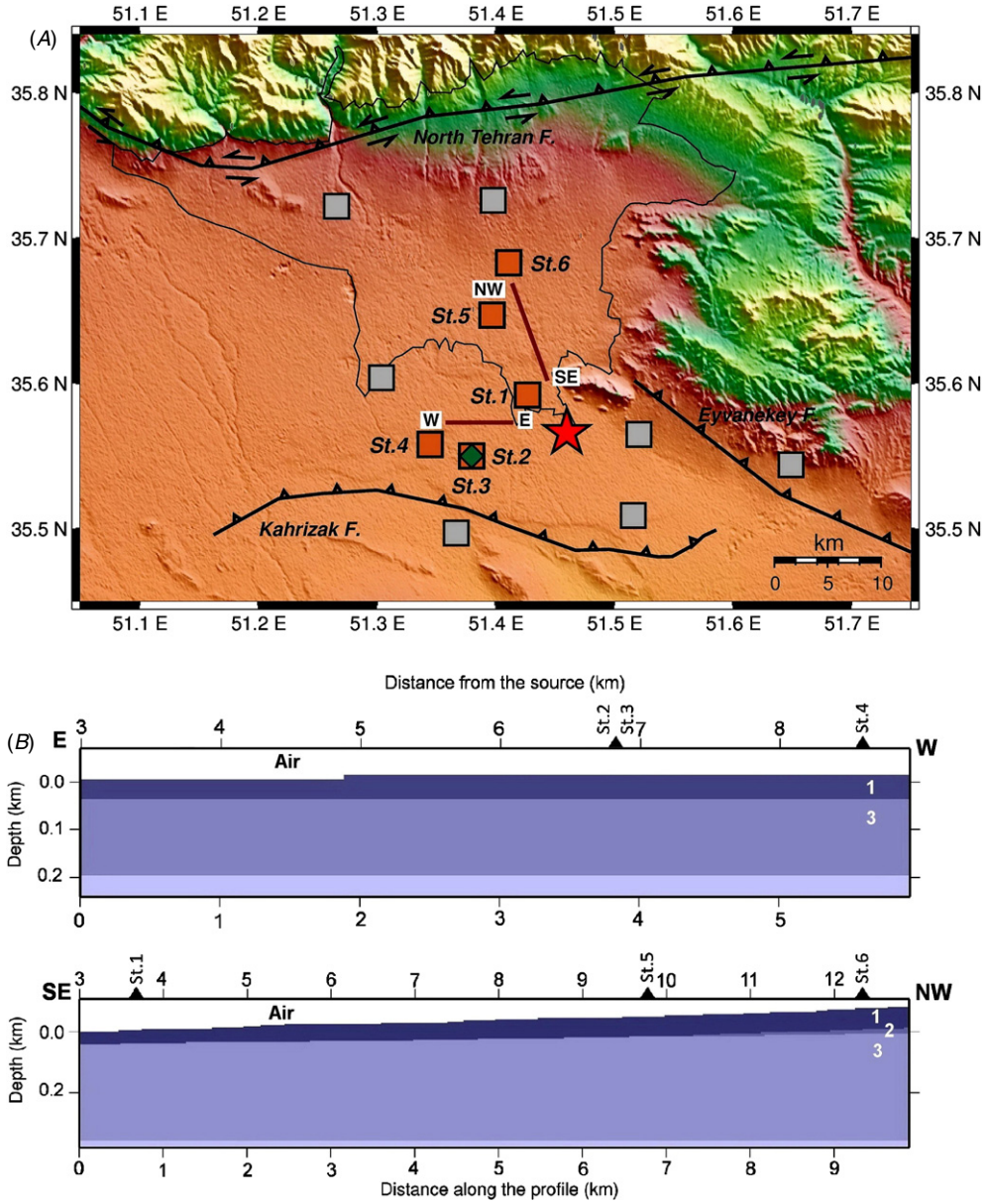

Figure 3. (*A*) Distribution of selected recording stations (labelled squares and diamond) from Building and House Research Center of Iran (BHRC) network for comparison between observed and synthetic data. Tehran city border is shown in thin black line and some major faults in thick black. The path of the two profiles (*B*), in the E–W and SE–NW directions, can be seen, along which the synthetic waveforms have been generated. Locations of stations (St.1 to St.6) are shown on profiles (*B*) and profile layers are separated by colour and numbers 1 to 3. The layers are defined in table 5 where the physical properties are introduced. The two lower profiles are the geometry of the local site models used in the hybrid method. The number of grid points in the finite difference computations is 700 $\times$ 165 for E–W and 2600 $\times$ 440 for SE–NW profile. The distances between the observation points and the source are of the order of 3–10 km for the E–W profile and 3–13 km for SE–NW profile.

Deformation and seismicity due to shortening in Iran accommodates the northward motion of the Arabian shield, southwest, towards the Eurasian plate, northeast. North–south shortening of 8 $\pm$ 2 mm yr^{-1} has been reported across Alborz range between central Iran and the southern Caspian shore (Vernant *et al* 2004).

Several active faults go across the Tehran city and its surroundings which emphasize the importance of seismic hazard in the region. North Tehran and Mosha faults and their westward continuation, the Taleghan fault, and Ipak, Eyvanaki, Garmsar and Pishva faults are some of the most important faults of the area. Figure 1 shows seismicity in the vicinity of Tehran based on International Institute of Earthquake Engineering and Seismology, IIEES, www.iiees.ac.ir, catalogue.

The distribution of historical earthquakes in the vicinity of Tehran shows that the region has been affected by eight large destructive earthquakes with magnitude greater than 7 from the 4th century BC to the present (Ambraseys and Melville 1982). The $M_W = 4.0$ earthquake occurred on 17 October 2009

Table 1. Location of earthquake reported by various agencies.

Agency	Latitude (deg)	Longitude (deg)	Depth (km)
IGTU	35.57	51.50	12
IIEES	35.50	51.57	18
TDMMO	35.55	51.53	16.8

at 10:53:57, GMT, in the southern part of Tehran. Although the earthquake was not strongly felt in Tehran, which hosts about 20% of the country's population, it nevertheless caused great concern, since the urban area of Tehran is developed on alluvial layers accumulated on hard rocks of complex geological formations (JICA 2000). Urban development has been rapidly progressing in Tehran without proper disaster prevention measures against the occurrence of very likely strong earthquakes. The strong historical earthquakes in the area of the city opposed to the present-day low level seismicity makes it necessary use to the few available good quality records in conjunction with advanced modelling methods, with the twofold purpose to calibrate the modelling with the scanty records on one side and to generate hazard scenarios, calibrated with the little available information, on the other. All this is necessary to implement reliable preventive actions, for the effective reduction of seismic risk of this important city. The 2009 earthquake provided data for testing the hybrid simulation method for Tehran. Evaluating a preventive hazard scenario by scaling extended source to higher magnitude and depth of historical events is the future plan of this study.

2. The 2009, $M_w = 4$, Tehran-Rey earthquake

The earthquake considered for simulation occurred in the south-eastern part of Tehran city and was felt in almost all parts of the city. An intensity of IV to III on the EMS98 scale has been estimated by the IIEES reconnaissance team (Farahani and Zare 2011). This earthquake was recorded by three seismographic networks (table 1): Institute of Geophysics of Tehran University (IGTU), Tehran Disaster Mitigation and Management Organization (TDMMO) (Yaminifard 2010, personal communication) and IIEES. The earthquake epicentre is located close to the Kahrizak and Eyvanekey faults, south and southeast of Tehran (figure 2). Stations of the IGTU and TDMMO networks are distributed appropriately in Tehran region. Reported epicentres by these two networks are very close and the difference, less than 3 km, is fully within the error bar of location, while they have a difference about 10 km with IIEES location. Hamzehloo *et al* (2009) observed a better match while determining the causative fault of the earthquake with the location of TDMMO, which is expected. TDMMO location is used for the source location in this study. The event was also recorded by Iranian strong motion network, operated by Building and House Research Center of Iran (BHRC). Figure 2 shows all stations of IGTU, IIEES, TDMMO and BHRC with the three different locations reported for the event.

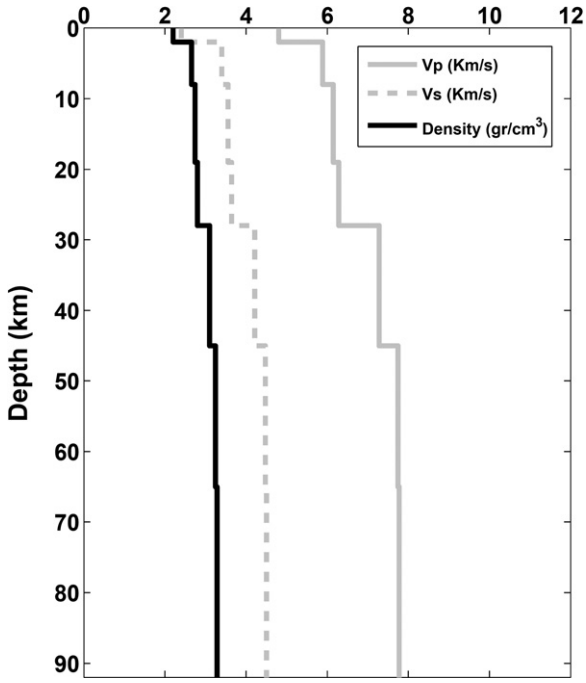

Figure 4. Velocity and density structures used for generating phase and group velocity of Rayleigh and Love waves with modal summation technique. This model, plus attenuation parameters, table 4, is used to propagate the waveform from the source to the close vicinity of the receiver.

Table 2. Parameters of two reported focal mechanisms for the earthquake.

Report	M_w	Strike (°N)	Dip (°)	Rake (°)	Depth (km)
Hamzehloo *et al* (2009)	4.0	292	36	59	16.8
Farahani and Zare (2011)	4.0	313	45	90	19.0

Source parameters of the earthquake, reported by Hamzehloo *et al* (2009) and Farahani and Zare (2011), are given in table 2.

3. Data

The 2009 earthquake was recorded by a total of 18 accelerographs of the strong motion array operated by BHRC, figure 2. Out of them, six stations (table 3 and figure 3) have been selected as the reference observed data set to be used in the comparison between recorded accelerograms and simulated ones. These six stations are close to the two profiles, cross-section, which are selected as simulation lines (figure 3). The main reasons to choose these profiles are the presence of subsoil information, covering both southern and central parts of the city which include the highest density of population, and are adjacent to the recording stations. The profiles extend in

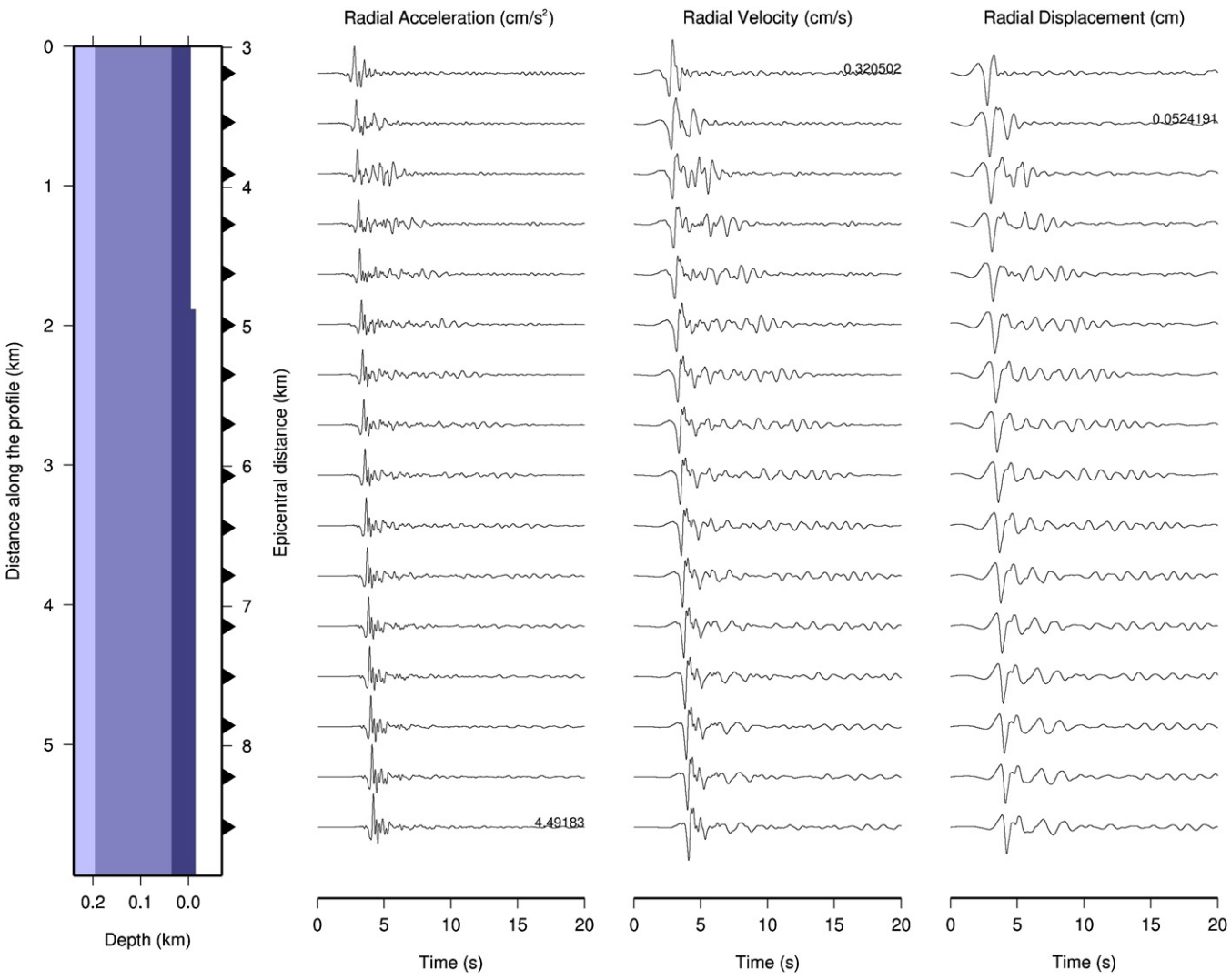

Figure 5. Acceleration, velocity and displacement time series for the radial component of synthetic signals along the E–W profile. Two different layers (down to 0.2 km) are shown with different colours; topography (height) is increasing slightly from east to west. Distance between sites where signals are computed along the profile surface is 60 m. Some generated signals (in steps of 6) are shown as they are computed along the profile. At the profile surface the receivers are represented by triangles. An elevation step of 10 m can be seen at distances of 2 km along profile. The topography is not severe except for a gradual rise in height. The profile is shown as what FD scheme sees and conducts propagating the wave. The late arrival of the first phase on synthetic signals is seen while passing from the starting point (top) to the end of profile (bottom). The peak value is shown on the pertinent seismogram.

Table 3. Building and House Research Center of Iran (BHRC) station names and locations used in this study.

BHRC station name	Station code used in this study	BHRC record number	Longitude (deg)	Longitude (deg)
Shahre Rey	St.1	4860	51.42	35.59
Haram Emam	St.2	4910	51.37	35.55
Haram Emam Borehole	St.3	4910B	51.37	35.55
Azad University	St.4	4867	51.34	35.55
Farhangsaraye Bahaman	St.5	4866	51.39	35.64
Park Shahr	St.6	4864	51.41	35.68

the East–West (E–W) direction, with a length of 6 km, and in the Southeast–Northwest (SE–NW) direction with a length of 10 km (figure 3). All stations recorded the three components, N–S, E–W and vertical, of motion with a sampling of 0.005 s. The station codes from St.1 to St.6 are assigned for Shahre Rey, Haram Emam, Haram Emam Borehole, Azad University,

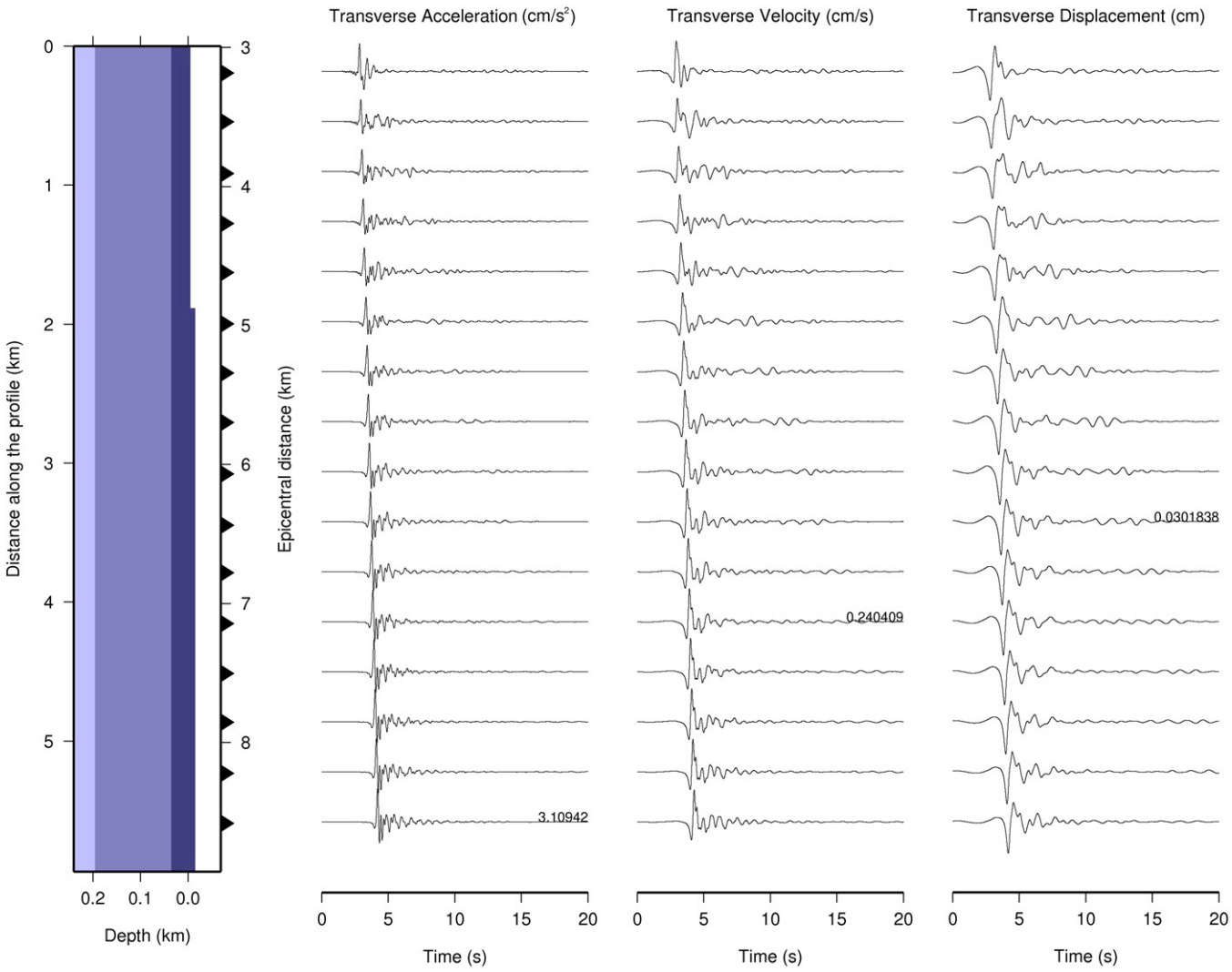

Figure 6. The same as in figure 5 for the transverse component of synthetic signals.

Farhangsaraye Bahman and Park Shahr, respectively. St.3 is located in a 30 m depth borehole under St.2 location (table 3 and figure 3).

4. Simulation method

A hybrid method developed by Fäh *et al* (1993a, 1993b) is used in this paper that combines the modal summation (MS) technique, valid for laterally homogeneous anelastic media, with finite difference (FD), which permits the modelling of wave propagation in complicated and rapidly varying velocity structures, as required when dealing with sedimentary basins, and optimizes the advantages of both methods. The method permits the accurate computation of the earthquake ground motion in two-dimensional (2D) laterally heterogeneous, anelastic media (Panza 1985, Panza and Suhadolc 1987, Florsch *et al* 1991, Fäh *et al* 1994, Panza *et al* 2001). Wave propagation is treated by means of the analytical modal summation technique in a laterally homogeneous anelastic structural model from the source to the close vicinity of the local, heterogeneous anelastic structure. The laterally homogeneous anelastic structural model, which includes quality factor, controlling the anelastic attenuation, velocity and density, represents the average crustal properties of the region and is considered as the bedrock reference model.

The wavefield generated by modal summation is then introduced in the grid that defines the heterogeneous area, for which the attenuation, velocity and density profiles must be specified, and it is propagated numerically according to the FD scheme (see figure 1 in Fäh *et al* (1994)). Explicit finite difference schemes are used here to simulate the propagation of seismic waves in the sedimentary basin and it requires at least ten grid points per wavelength (e.g. Alford *et al* 1974). This limits the maximum size of the structural local model, but allows the modelling of complicated and rapidly varying velocity structures. These schemes are based on the formulation of Korn and Stöckl (1982) for

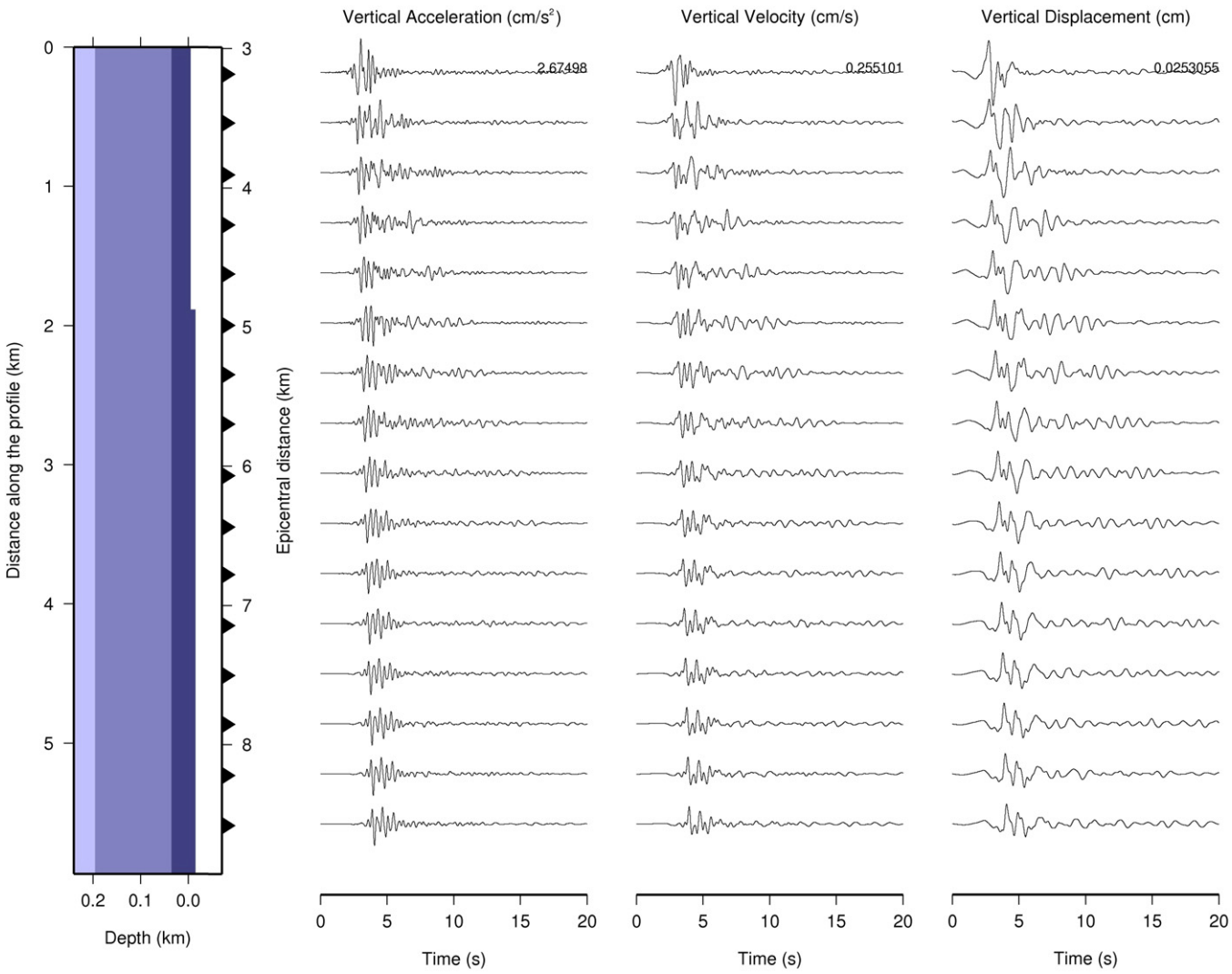

Figure 7. The same as in figure 5 for the vertical component of synthetic signals.

SH waves, and on the velocity-stress, finite difference method for P-SV waves (Virieux 1986). The schemes are stable for materials with high, as well as normal values of Poisson's ratio.

Through this hybrid approach, source, path and site effects are all taken into account. It is therefore possible to carry out a detailed study of the wavefield that propagates at large distances from the epicentre. This hybrid approach has been successfully applied and verified for the purpose of simulation and seismic microzoning in several urban areas like Mexico City, Rome (Fäh and Panza 1994), Benevento (Fäh and Suhadolc 1995, Marrara and Suhadolc 1998), Naples (Nunziata *et al* 1995), Tehran (Hamzehloo *et al* 2007) and Catania (Romanelli *et al* 1998b, 1998a) in the framework of the IUGS-UNESCO-IGCP project (Panza *et al* 1999). For a detailed description of theory and method, see Panza *et al* (2001).

5. Structural model parameters

There are two stages of wave treatment in this hybrid modelling. The first, from the source to the close vicinity of the site, is treated with MS and needs a regional structure model. Then the output of the first stage propagates through a grid area of local site to the surface, which is treated with a FD approach and needs a local (basin) structure model. Both these models are characterized with velocity, density and attenuation parameters in regional and local scales, respectively. The reference, 1D, layered model of the crust and upper mantle for the first stage has been obtained from Rahimi (2010) and is shown in table 4 and figure 4. The local models for the FD scheme are given in table 5 and figure 3. The geometry of the two profiles in E–W and SE–NW directions has been retrieved from the literature (JICA 2000) and geological cross sections of Geology Survey of Iran (GSI), www.gsi.ir. The parameters and physical properties (table 5) for local 2D models are

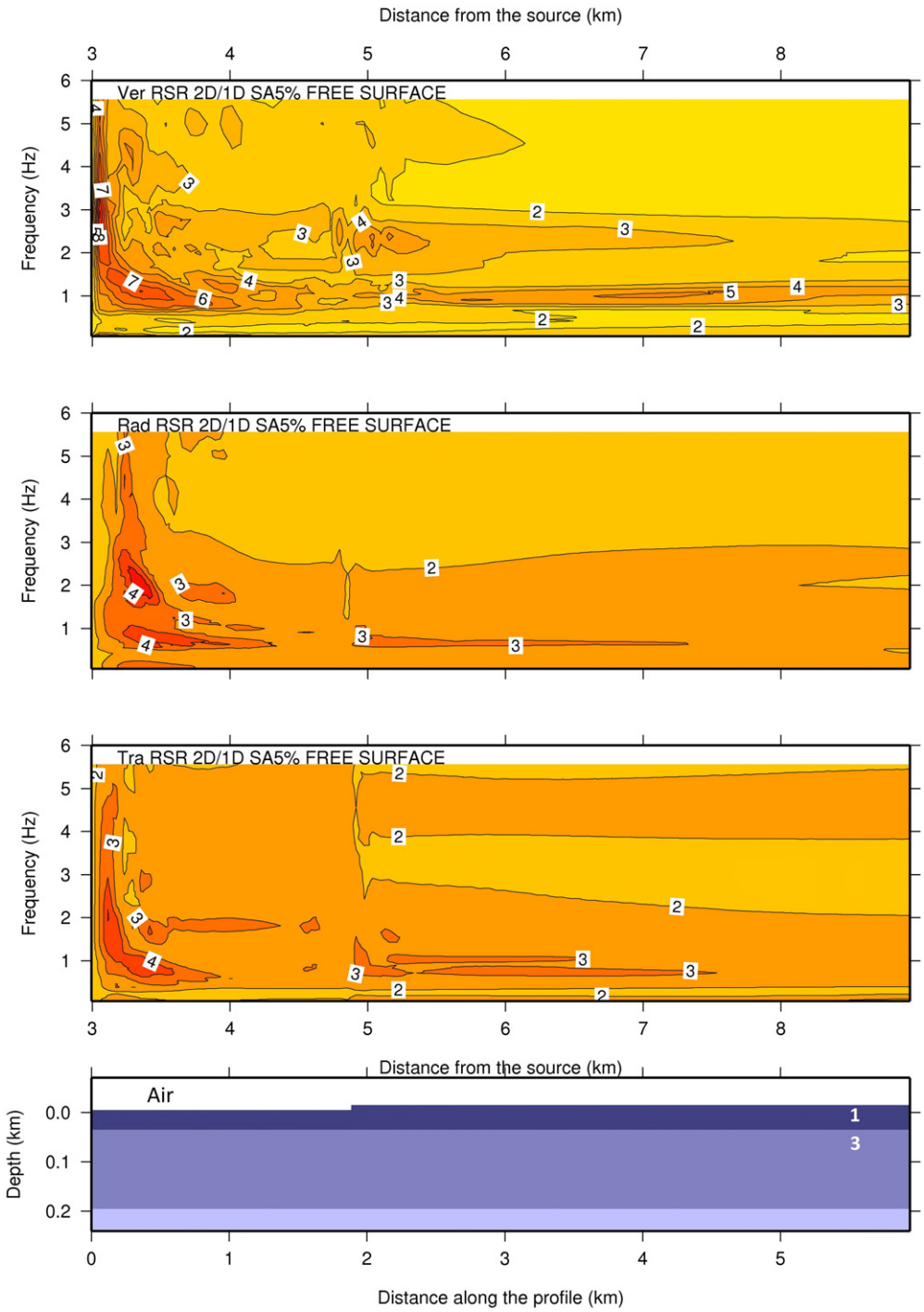

Figure 8. Response spectral ratios (RSR) (damping 5%) for the vertical, radial and transverse components of synthetic signals along the entire E–W cross section. For each receiver point at the surface (triangles in figures 5–7), response spectra of two seismograms, one with and the next without the effect of local site, are computed and the ratio is calculated, and then the contour map is prepared along the profile. The numbers on the figure show simply the amplification imposed by the local site.

obtained from Hamzehloo *et al* (2007). Although the method has the potential to be applied in very complex basins, in this case the profiles do not include such complexity except for a rise in elevation which can be seen in part (*B*) of figure 3. The epicentral distance from source to the closest point of the profiles is about 3 km. The location of selected observing stations along profiles is shown in figure 3.

6. Results

The hybrid technique has been applied to generate synthetic signals along the two profiles shown in figure 3. The six recording stations closest to the profiles have been selected for comparison and test of the reliability of synthetic data. For each

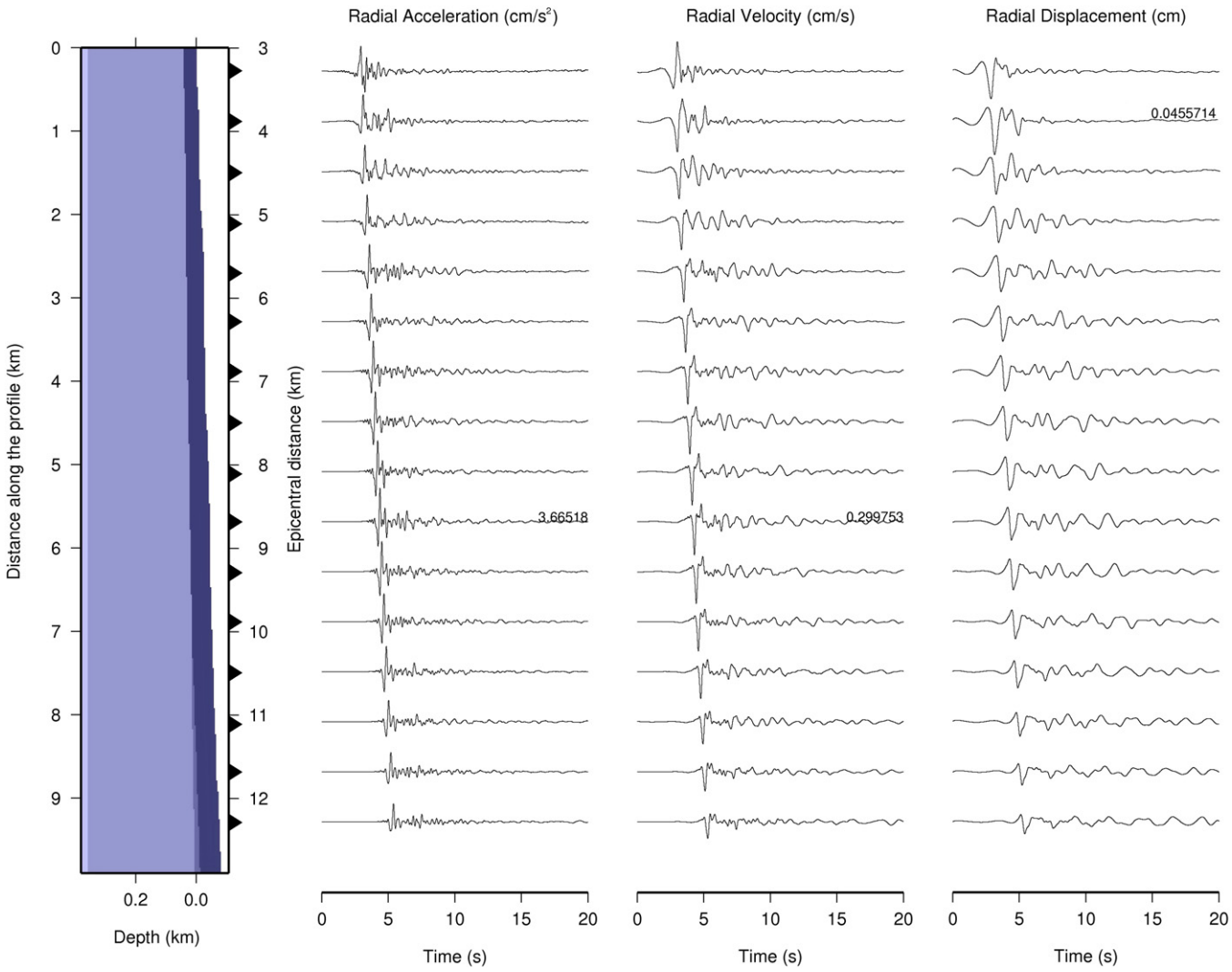

Figure 9. The same as in figure 5 for the radial component of synthetic signals for the SE–NW profile. Three different layers are shown with different colors; topography (height) is increasing from SE to NW and a thin layer starts at the end parts of profile. The distance between sites where signals are computed along the profile surface is 100 m.

Table 4. Structural regional reference model of crust and upper mantle, over a half space, used with modal summation technique.

Layer thickness (km)	Density (g cm^{-3})	V_P (km s^{-1})	V_S (km s^{-1})	Q_P	Q_S	Bottom depth (km)	Layer
2	2.20	4.80	2.40	264	120	2	1
6	2.66	5.89	3.40	264	120	8	2
11	2.74	6.15	3.56	264	120	19	3
9	2.78	6.29	3.64	264	120	28	4
17	3.10	7.28	4.21	330	150	45	5
20	3.25	7.75	4.48	330	150	65	6
27	3.29	7.78	4.50	330	150	92	7

station, earthquake ground motion acceleration, velocity and displacement have been generated as time domain parameters and absolute acceleration response spectra and response spectral ratio between 2D and 1D signals are calculated as frequency domain parameters.

For the FD computation along the E–W profile, a grid of 700 by 165 points, along the X and Z axis, respectively, has been used while for SE–NW profile the grid is 2600 (X) by 440 (Z) points. The grid step is 0.01 km for the E–W profile and 0.004 km for the SE–NW profile. The SE–NW profile

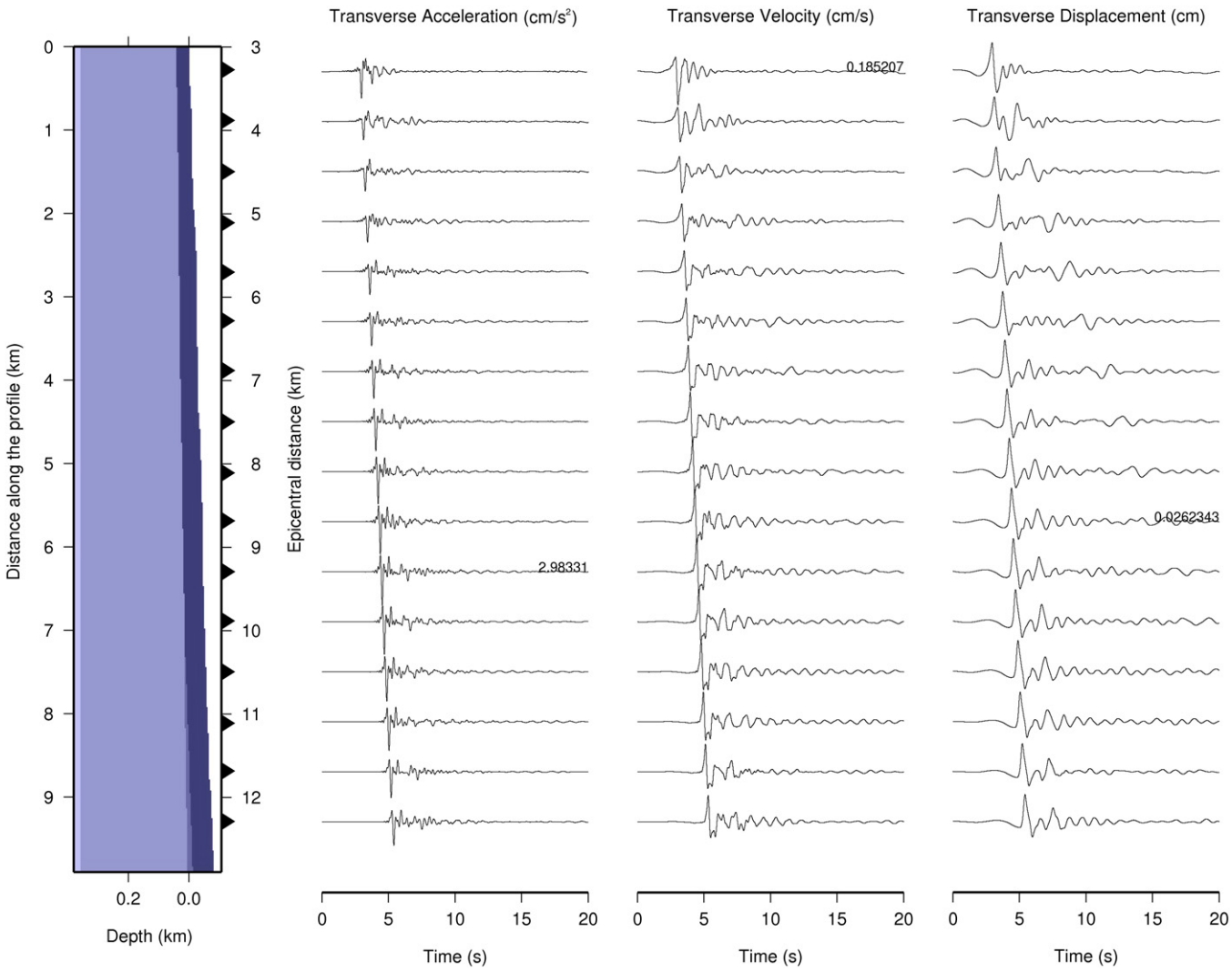

Figure 10. The same as in figure 9 for the transverse component of synthetic signals, SE–NW profile.

Table 5. Physical properties of the cross sections along the local profiles.

Layer formation	Density (g cm^{-3})	V_P (km s^{-1})	V_S (km s^{-1})	Q_P	Q_S	Layer
Silt and clay	1.7	0.5	0.25	88	40	1
Kahrizak formation (young alluvial deposits)	1.8	0.8	0.5	88	40	2
Conglomerates with a few lenses of sandstone, siltstone and mudstone	1.9	1.1	0.6	88	40	3

includes a thin layer (figure 3, layer 2), which needs a smaller grid point to detect via this method. Since we need at least ten points of the grid per wavelength in the FD computation, then the shortest wavelength is obtained considering the lowest V_s and the highest frequency as $\lambda = V_s(\min)/F(\max)$. Given that usually in FD schemes the number of grid points is limited, there is always a trade-off between the model size and the maximum frequency that seems appropriate for the problem. In our case, the lowest V_s is 0.25 km s^{-1} and the maximum frequency 5.4 Hz gives the possibility to manage wavelengths very smaller than what we usually encounter in seismology. The signals are computed with a cutoff frequency of 10.0 Hz and filtered down to frequencies less than 6 Hz. The waveforms are scaled to the desired magnitude in the frequency domain using the scaling law of Gusev (1983) as reported by Aki (1987).

Figures 5–7 show the synthetic signals along the E–W profile and figures 9–11 give the same information for the

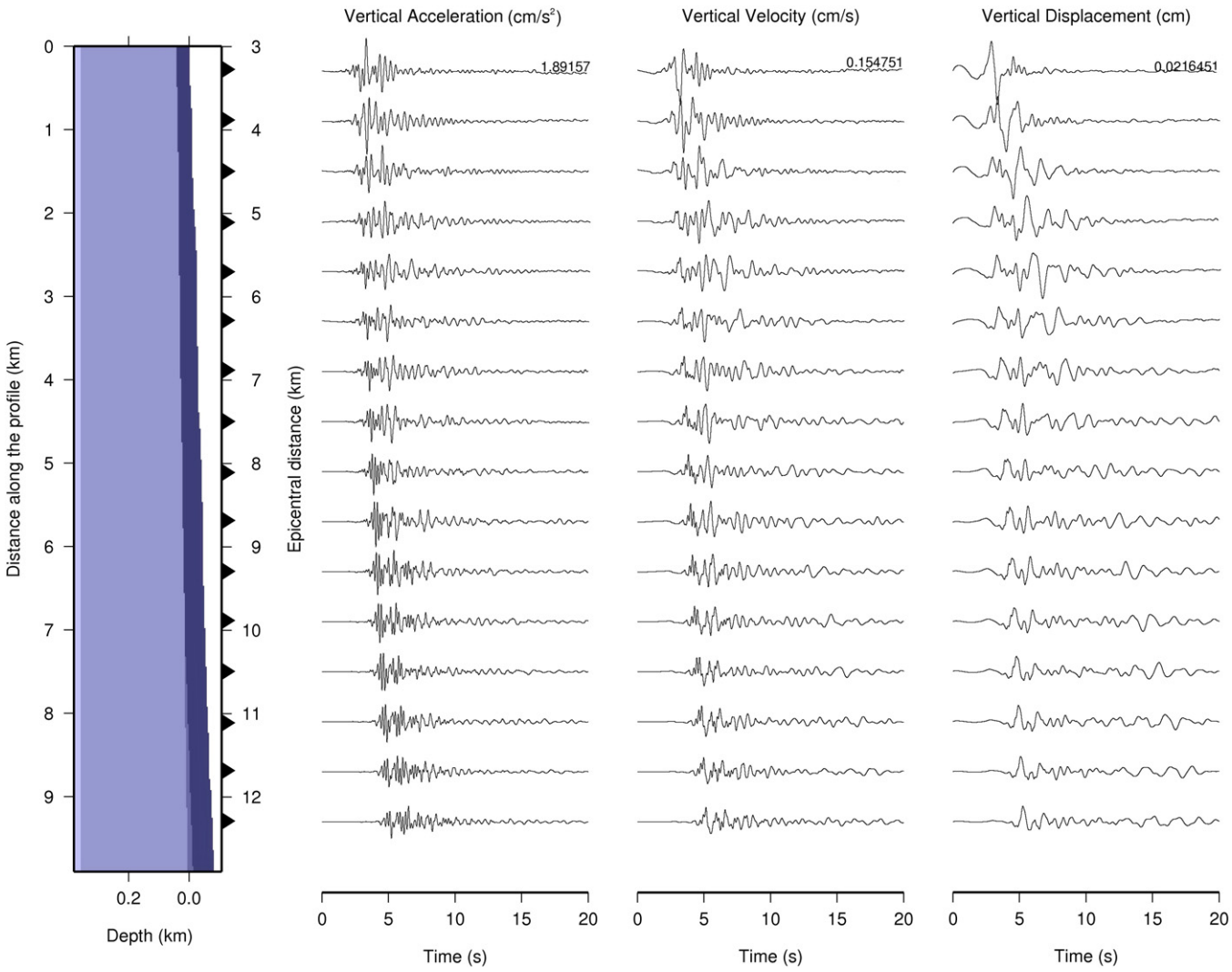

Figure 11. The same as in figure 9 for the vertical component of synthetic signals, SE–NW profile.

SE–NW profile. The distance between the receivers created during the modelling is 60 m for the E–W profile and 100 m for the SE–NW profile that for better view are plotted with a skipping of 6 in figures 5–7 and 9–11. Peak values of acceleration (cm s^{-2}), velocity (cm s^{-1}) and displacement (cm) are shown, in the figures, close to the pertinent signal. The synthetic signals explain the major characteristics of the observed ground motion along these two profiles. As can be seen, arrival times, as expected, are delayed moving from the beginning of the models to the end, top to bottom. Using such a technique, a complete waveform data bank is generated which can be the base for realistic hazard estimation. Triangles on the profiles, in figures 5–7 and 9–11, show the assumed receivers.

The surface topography is considered but generally topography and basin geometry are not severe and complicated, especially in E–W profile. Therefore, the main difference between the signals along the array is the decrease or increase in amplitude due to geometrical spreading and attenuation or due to local site effect. The long tails which are usually seen in very heterogeneous basins are not so clear for the E–W profile, while for SE–NW they are clearer and the signals are longer in the tail to the end of profiles.

In general, a representation of local site effects (amplification) is given by the computation of spectral ratios between the signals obtained (1) with insertion of the local models (table 5 and figure 3) of the sedimentary basin, and (2) with a reference model in which the upper few hundred metres of the basin are replaced by the first layer of one-dimensional structure, presented in the regional model (table 4 and figure 4). Both signals have in common the source and the path, so that from the spectral ratios the effects of the sedimentary basin are clearly exhibited. In other word, the resulting time domain signals are used for local seismic microzoning, using as zoning criteria the 'response spectra ratio' (RSR), i.e. the spectral amplification defined by RSR = [Sa(2D)/Sa(1D)] where Sa(2D) is the response spectrum, at 5% of damping, for

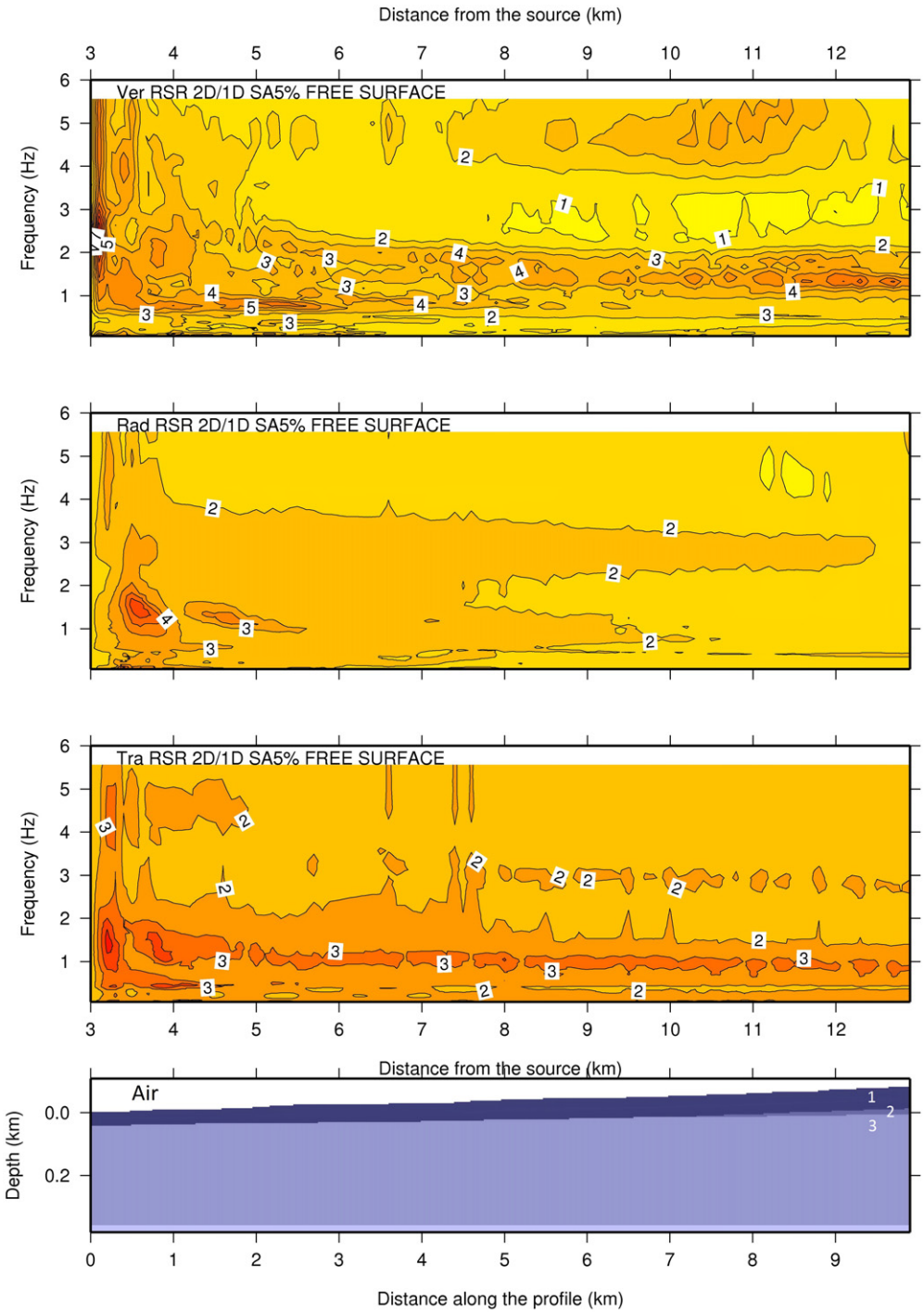

Figure 12. The same as figure 8 for SE–NW profile.

the signals calculated in the laterally varying structure (local profile), and Sa(1D) is the one calculated for signals at the top of the counterpart bedrock regional reference structure (beneath the local profile). Site amplification estimated in terms of RSR for the two profiles is shown in figure 8, E–W, and figure 12, SE–NW.

From the created data bank of synthetic seismograms the closest ones to the selected recording stations are extracted for comparison. Peak values of observed and synthetic data are given in tables 6 and 7, while waveforms of related observed and synthetic seismograms are shown in figures 13–15, for the various stations and components. All observed and synthetic seismograms are filtered and normalized to the same amplitude. Instrumental response is removed from seismograms.

Response spectra of observed and related synthetic signals are compared in figure 16. Comparison between the observed ground motion and the synthetic signals (figures 13

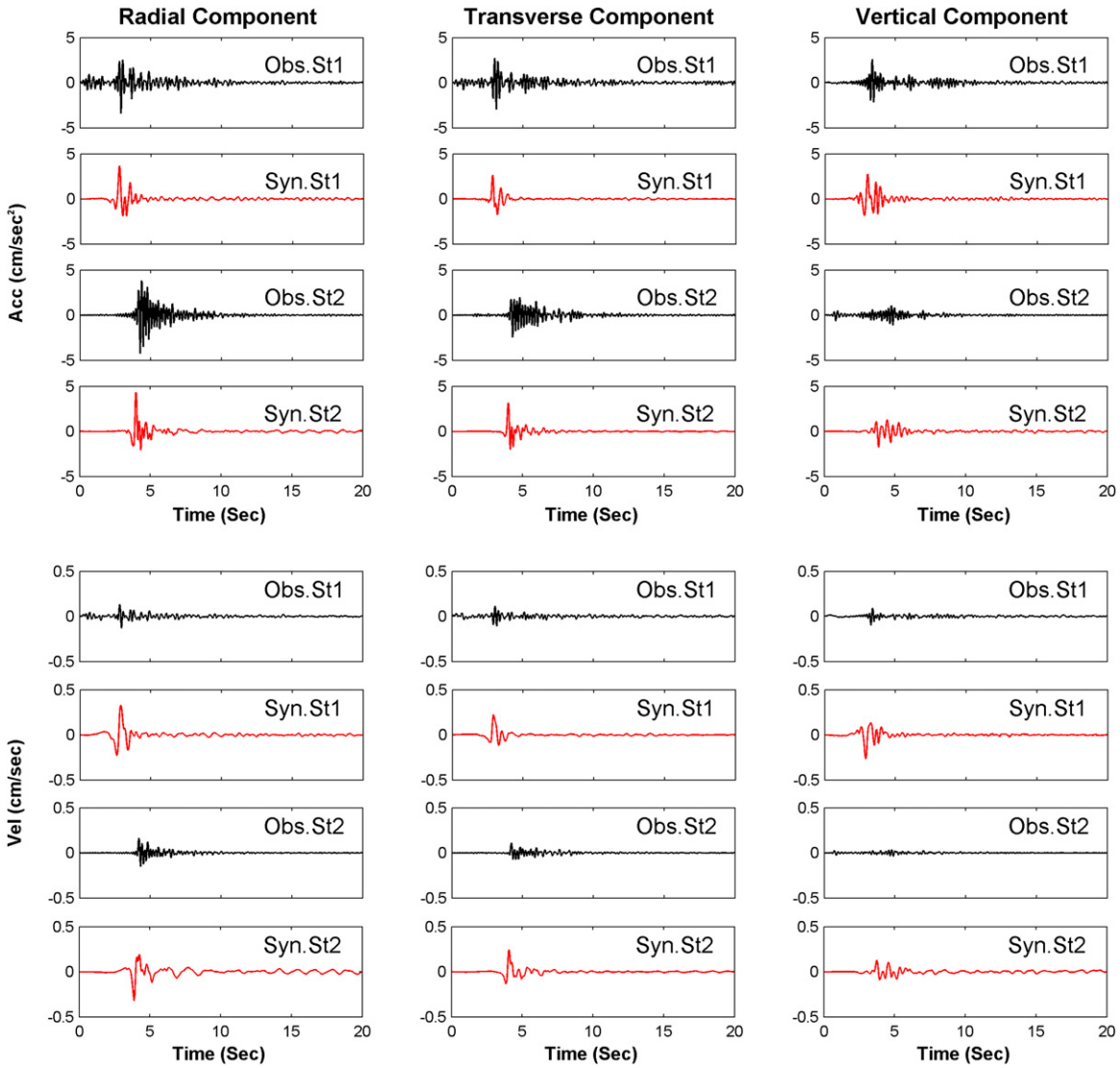

Figure 13. Observed (black) and synthetic (coloured) waveforms of acceleration (cm s^{-2}) (top) and velocity (cm s^{-1}) (bottom) for stations 1 and 2. For synthetic waveforms, the closest generated signal along the profile to the real recording station is extracted and used. Synthetic signals, same filtered as observed between 0.1 and 5.4 Hz.

Table 6. Comparison of peak ground acceleration (PGA) of observed and synthetic seismograms. Station names inside parentheses are taken from the Building and House Research Center of Iran.

	Radial comp. PGA (cm s^{-2})		Transverse comp. PGA (cm s^{-2})		Vertical comp. PGA (cm s^{-2})	
Station	Obs.	Syn.	Obs.	Syn.	Obs.	Syn.
St.1 (Shahre Rey)	3.36	3.60	2.95	2.65	2.59	2.68
St.2 (Haram Emam)	4.20	4.10	2.42	2.90	1.08	1.60
St.3 (Haram Emam Borehole)	2.38	1.90	0.62	1.15	0.19	0.60
St.4 (Azad University)	3.52	4.00	3.39	3.10	1.25	1.60
St.5 (Farhangsaraye Bahman)	3.69	3.50	2.83	2.99	1.93	1.33
St.6 (Park Shahr)	1.34	1.90	2.83	2.19	0.78	0.75

to 15), due to the variability of strong ground motion within the sedimentary basin, the poorly known structure of the sedimentary basin in Tehran and the fact that none of the accelerometric stations is located exactly on the profiles studied, it is difficult to capture all the observed features with the highest accuracy.

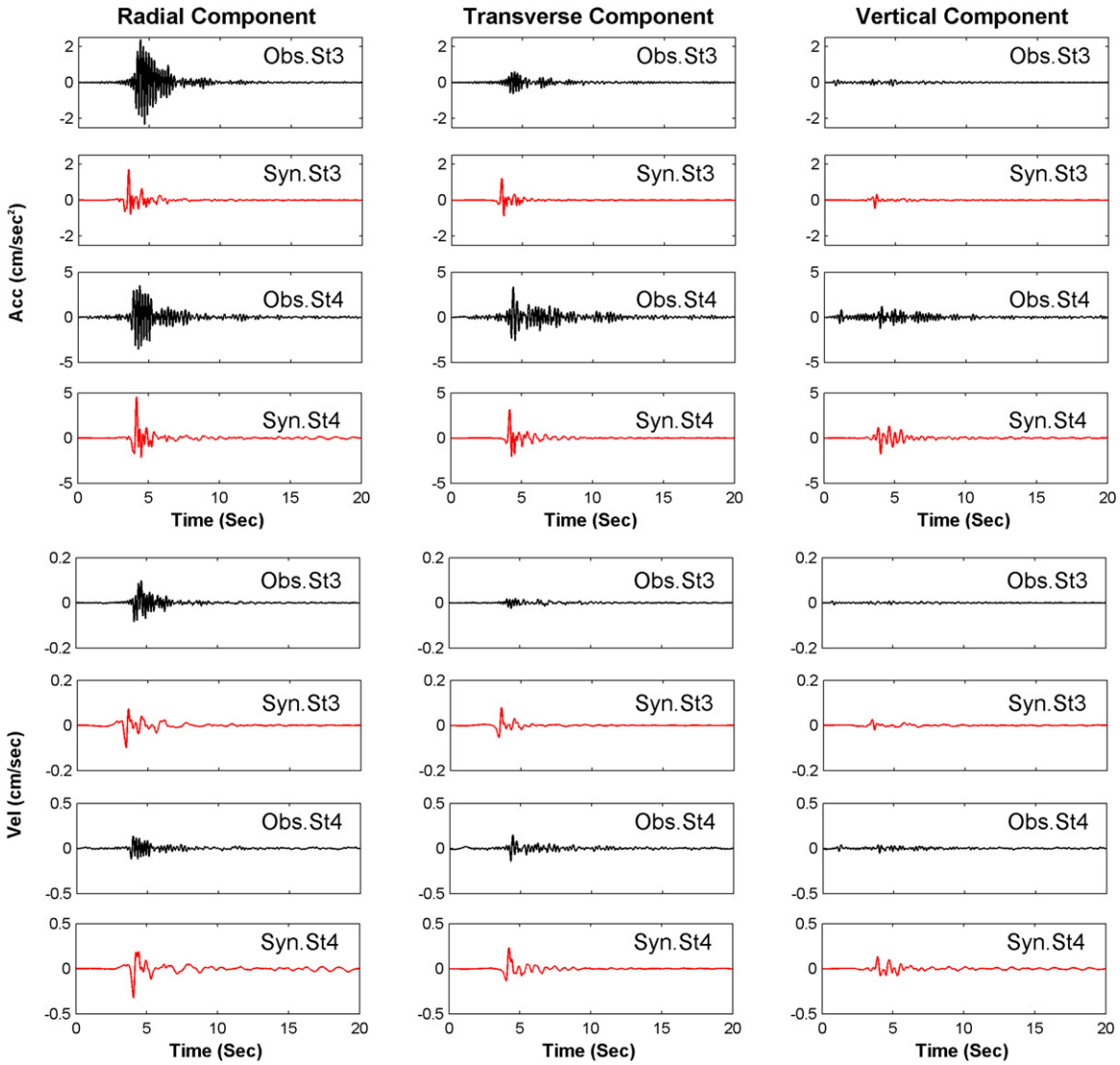

Figure 14. The same as in figure 13 for stations 3 and 4.

Table 7. Comparison of peak ground velocity (PGV) of observed and synthetic seismograms. Station names inside parentheses are taken from the Building and House Research Center of Iran.

	Radial comp. PGV (cm s^{-1})		Transverse comp. PGV (cm s^{-1})		Vertical comp. PGV (cm s^{-1})	
Station	Obs.	Syn.	Obs.	Syn.	Obs.	Syn.
St.1 (Shahre Rey)	0.13	0.31	0.11	0.18	0.09	0.20
St.2 (Haram Emam)	0.16	0.29	0.11	0.22	0.03	0.09
St.3 (Haram Emam Borehole)	0.09	0.09	0.02	0.01	0.01	0.01
St.4 (Azad University)	0.13	0.20	0.15	0.22	0.05	0.09
St.5 (Farhangsaraye Bahman)	0.13	0.23	0.15	0.20	0.07	0.08
St.6 (Park Shahr)	0.05	0.09	0.13	0.12	0.03	0.03

A parametric study is performed that demonstrates the sensitivity of computed ground motion to changes in the source parameters of depth, rake and dip. Figures 17–19 show results on how the peak acceleration changes with changing source parameters for various epicentral distances (edi). Results are prepared for two source–receiver angles (the angle between the strike of the fault and the direction obtained connecting the epicentre with the station, measured anticlockwise, see Panza

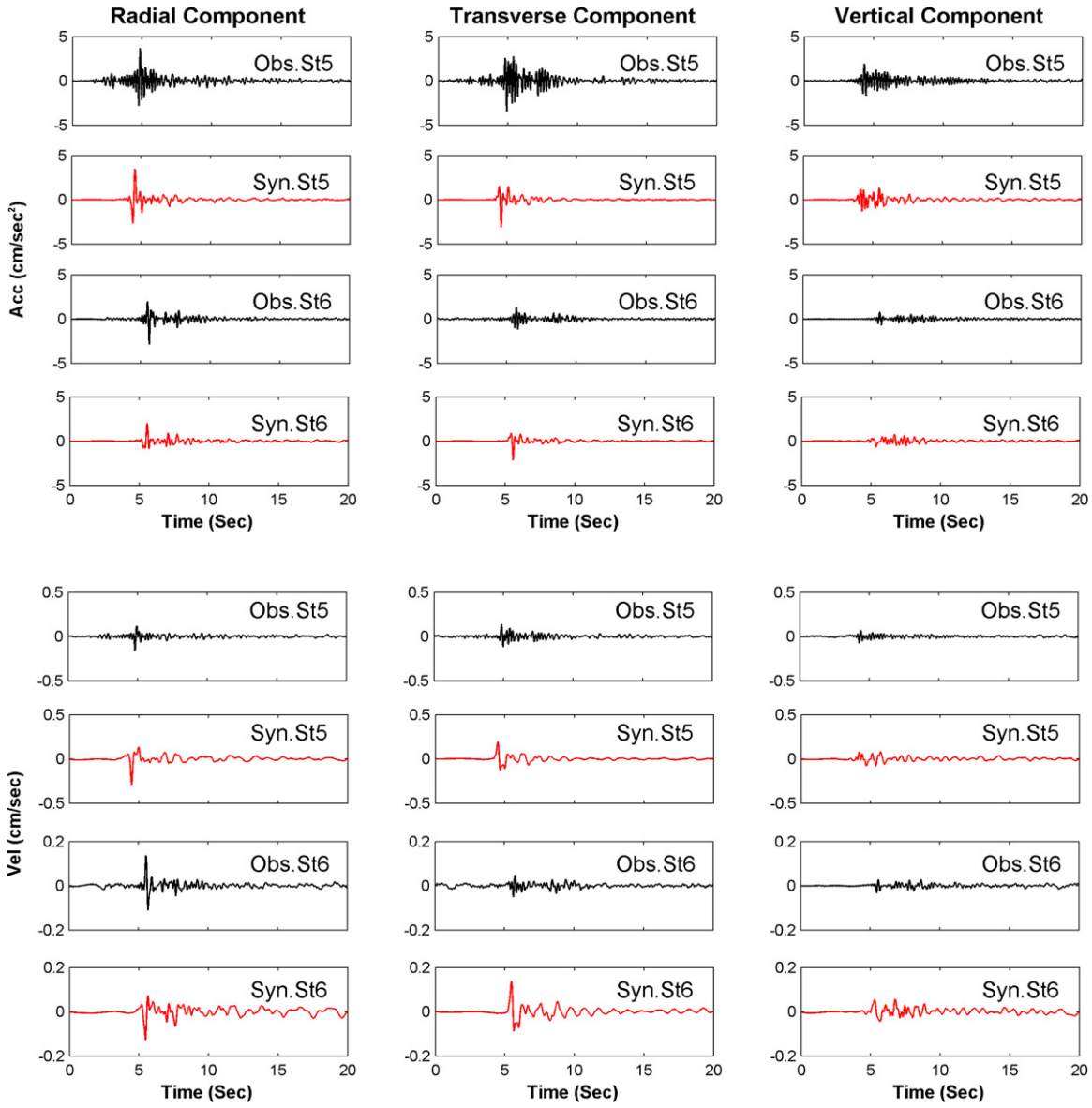

Figure 15. The same as in figure 13 for stations 5 and 6.

et al 2001) of E–W and SE–NW profiles. They clearly show how the various parameters can affect the peak acceleration and are the basis for defining an earthquake scenario with the highest level of danger while evaluating hazard for an area. The results of parametric study are calculated for all radial, transverse and vertical components.

Another parametric study is done considering the sensitivity of synthetic seismograms to 10% changes, increasing and decreasing, in the physical properties (V_s, V_p, Q_s, Q_p) of the sedimentary basin (table 5). Figure 20 shows the result for station 5 and other stations show similar behaviour. Four step changes are done. Two steps relate to attenuation values, 10% decreasing and increasing, and two steps to velocity values, 10% decreasing and increasing. The results, same filtered as observed between 0.1 and 5.4 Hz and plotted at the same scale and the values of maximum amplitude for each signal are shown. It shows how the signals, created by the model from the literature, changes while the physical properties are changing 10%.

7. Discussion

Ground motion simulation of the 2009, $M_w = 4$ earthquake southeastern of Tehran metropolis has been performed taking simultaneously into account the source, path and site effects. The comparison between observed and synthetized signals shows good agreement on account of the fact that no data fitting is made, but only literature data are used as input. The accordance is seen both in time

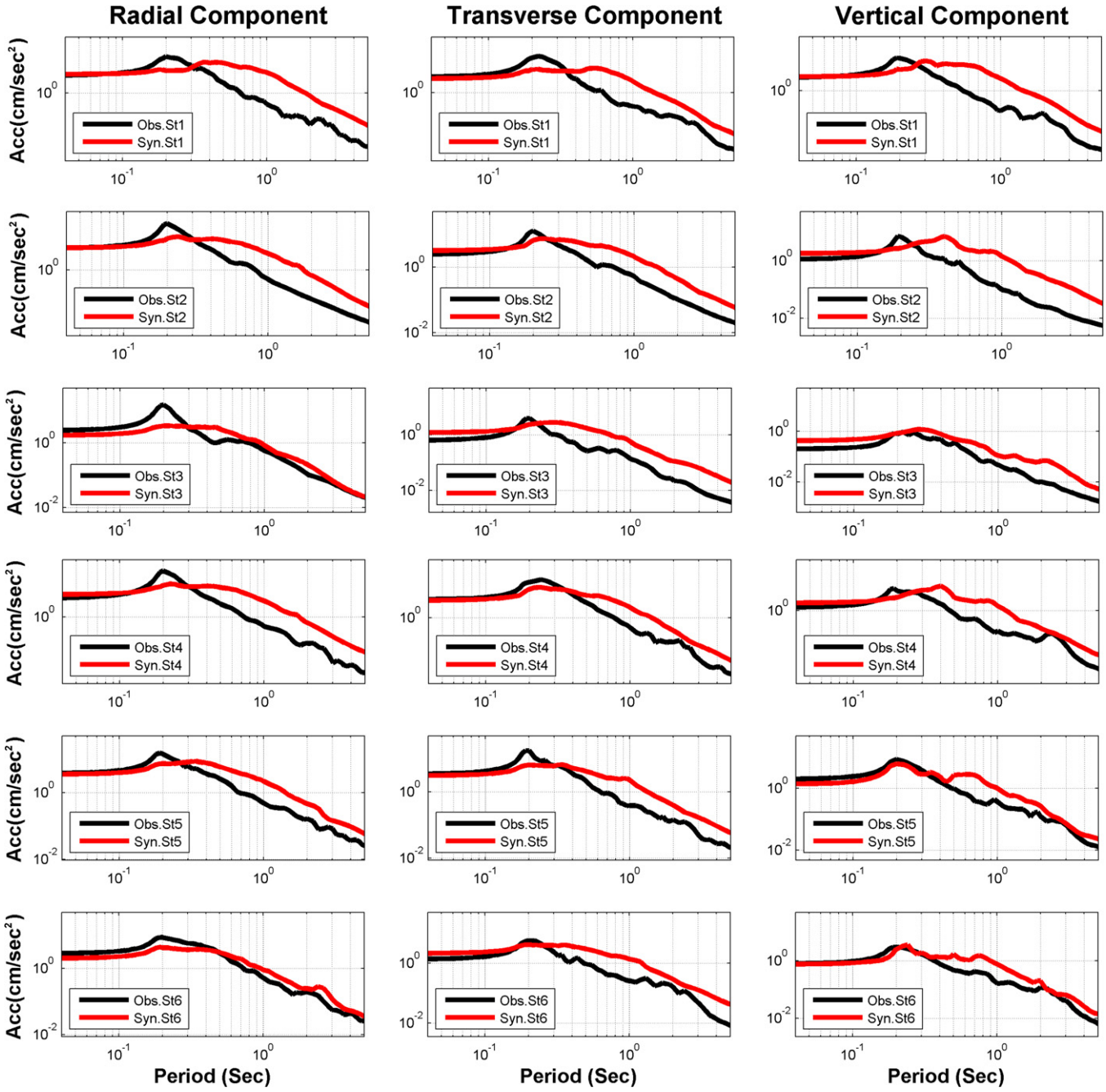

Figure 16. Observed (black) and synthetic (coloured), response spectra (5% damping) for stations 1 to 6. No data fitting is performed and a wide band of frequency (0.1–5.4) is selected.

and frequency domain, where we have compared PGA, PGV and response spectra of observed and simulated data.

In the time domain, quite good agreement is seen between observed and simulated PGA (table 6) and acceptable agreement in PGV (table 7). The observed differences should be related to the ambiguity and uncertainties of some basic information on local structure geometry, physical and attenuation parameters. Results show that in spite of the absence of some localized information about lateral variations of attenuation and velocity parameters for subsurface layers, the known values of the structural parameters have allowed us to capture some of the interesting features of the ground motion. Definitely 3D models and simulations are able to capture more details of observed data but in our case they were not available and for many areas even 2D models are rarely available. Although it is possible to make more adjustment between observed and synthetic

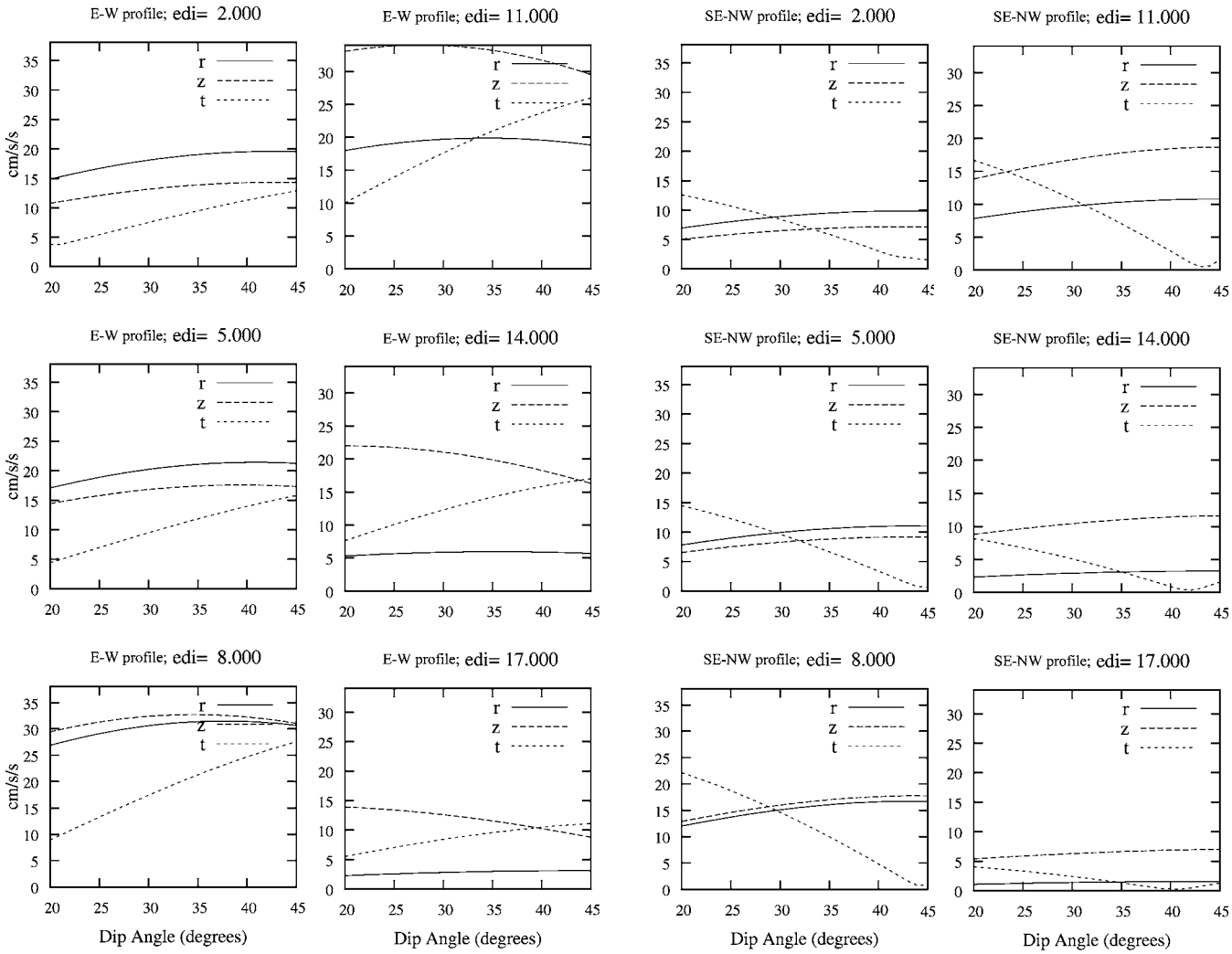

Figure 17. Parametric study on dip of the source to demonstrate the sensitivity of computed ground motion to small changes in dip along E–W and SE–NW profiles. The parametric test is performed for various epicentral distances (edi) of 2–17 km with steps of 3 km. The two columns on the left are assigned for E–W and the two on right for the SE–NW profile. The peak amplitudes of created seismograms are calculated while changing the dip angle around reported values and the figure is prepared. It shows how the amplitudes vary if the source dip varies around reported values, table 2.

signals by more runs and iteration, the results obtained so far are very important for preventive actions made using synthetic data and enable us to prepare a fine data bank of synthetic data considering the physics of the earthquake.

Generally, the whole shape of seismograms, with slight changes in source parameters or local model properties, is rather stable, while amplitudes increasing or decreasing are almost are negligible (figures 17–20). Earlier and later arrivals are expected with changing velocity, as can be seen in figure 20. Local soil conditions and irregular geological structures can significantly affect the characteristics of ground motion during earthquakes. Despite the difficulties in modelling such effects, they should not be ignored in the assessment of seismic hazard or in zonation studies. In general, the structural models used in theoretical studies of the seismic response of sedimentary basins are chosen to be very simple. They usually consist of a homogeneous half-space with sedimentary basins modelled by overlying sequences of layers. The velocity contrast between the basins and the half-space is chosen to be quite large in order to emphasize the main effects of the basins. The seismic response of such structures is then calculated, rather schematically, by assuming a plane incident wavefield. Studies of this sort have shown the well-known amplification of the incident plane waves, which occurs when a seismic wave travels through an interface from a medium with relatively high rigidity, into a medium of lower rigidity. The presence of a sedimentary cover of several tens of metres implies that the sedimentary basin can have a large influence on wave propagation. This effect is studied here with the hybrid approach and represents an application of this technique for amplification prediction. Estimation of local site effect in terms

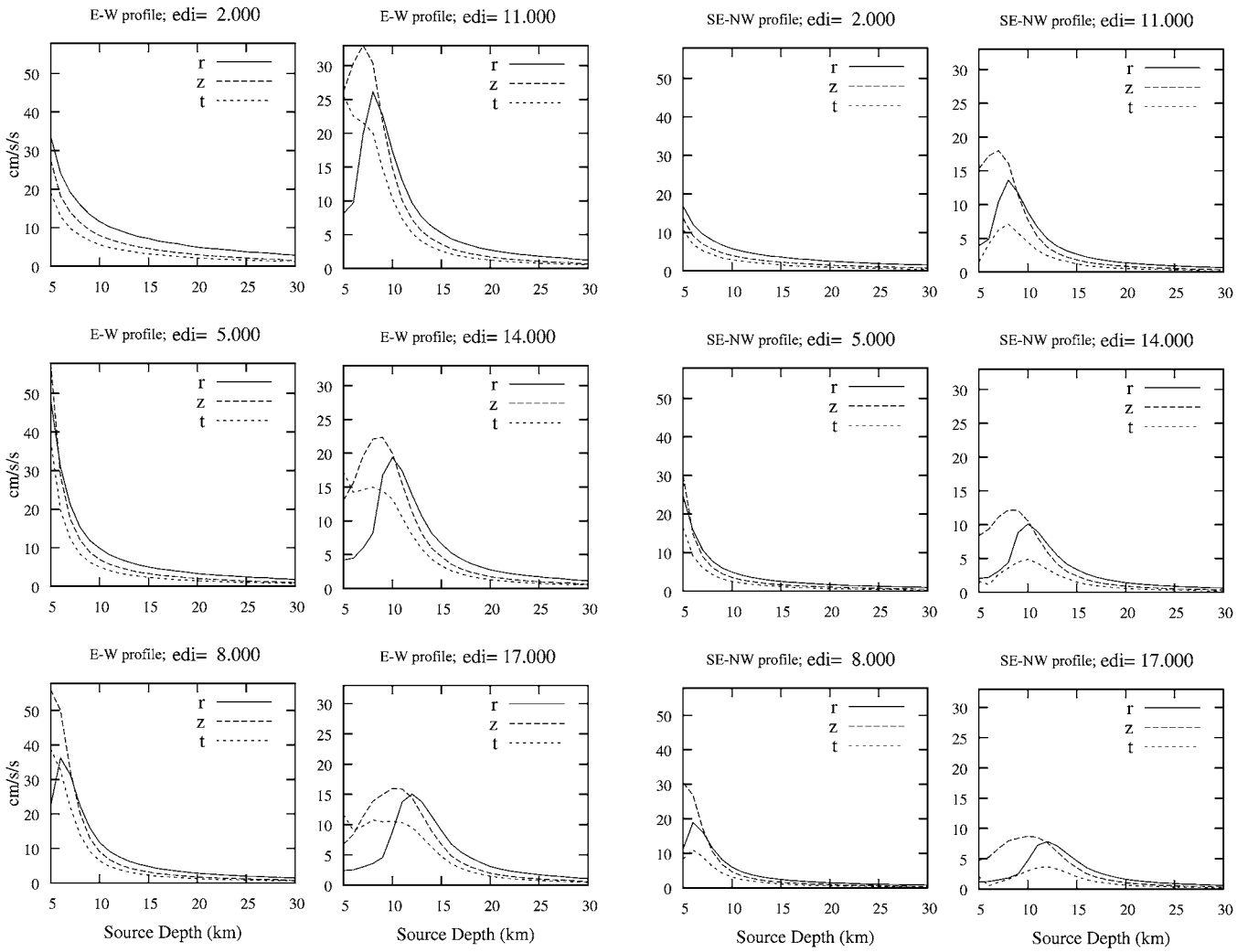

Figure 18. The same as in figure 17 considering the depth of the source.

of response spectra ratios, in spite of the very simple available geometry of the subsurface layers, shows the relevant effect the Quaternary sediments. The amplification level reaches 6 in some areas (figures 8 and 12), in good agreement with the results obtained by Haghshenas (2005) and Hamzehloo *et al* (2007).

Both reported mechanisms have been used as input values without any data fitting. The solution of Hamzehloo *et al* (2009) shows better agreement when the average root-mean-square, RMS, error of response spectra for all six stations is calculated between observed and simulated data. The RMS corresponding to Hamzehloo *et al* (2009) mechanism is 0.32 while for Farahani and Zare (2011) the value is 0.49. The reason could be addressed to a combination of source, path and site effects which definitely affect the modelling procedures in both methods.

While lots of simulation methods only provide a limited band of low or high frequency parts of the signal, the wide-band, 0.1–5.4 Hz, synthetic signals that take into account source characteristics, path and local geological and geotechnical conditions have been produced at a very low cost/benefit ratio.

8. Conclusion

Lack of detailed available data from basin geometry causes some discrepancies between observed and synthetic signals. In our case, unavailability of data applies to almost all physical parameters of the basin layers, i.e. velocity, density and attenuation. This has caused slight different shapes, duration and frequency content; due to these, the available models could predict engineering parameters with fairly reliable values in amplitude and frequency parameters. Checking out the observed and synthetic seismograms from outputs of two reported focal mechanisms shows that the Hamzehloo *et al* (2009) data are closer to reality as they cause lower RMS. Based on parametric tests it can be understood that the method and outputs are stable while changing reference values

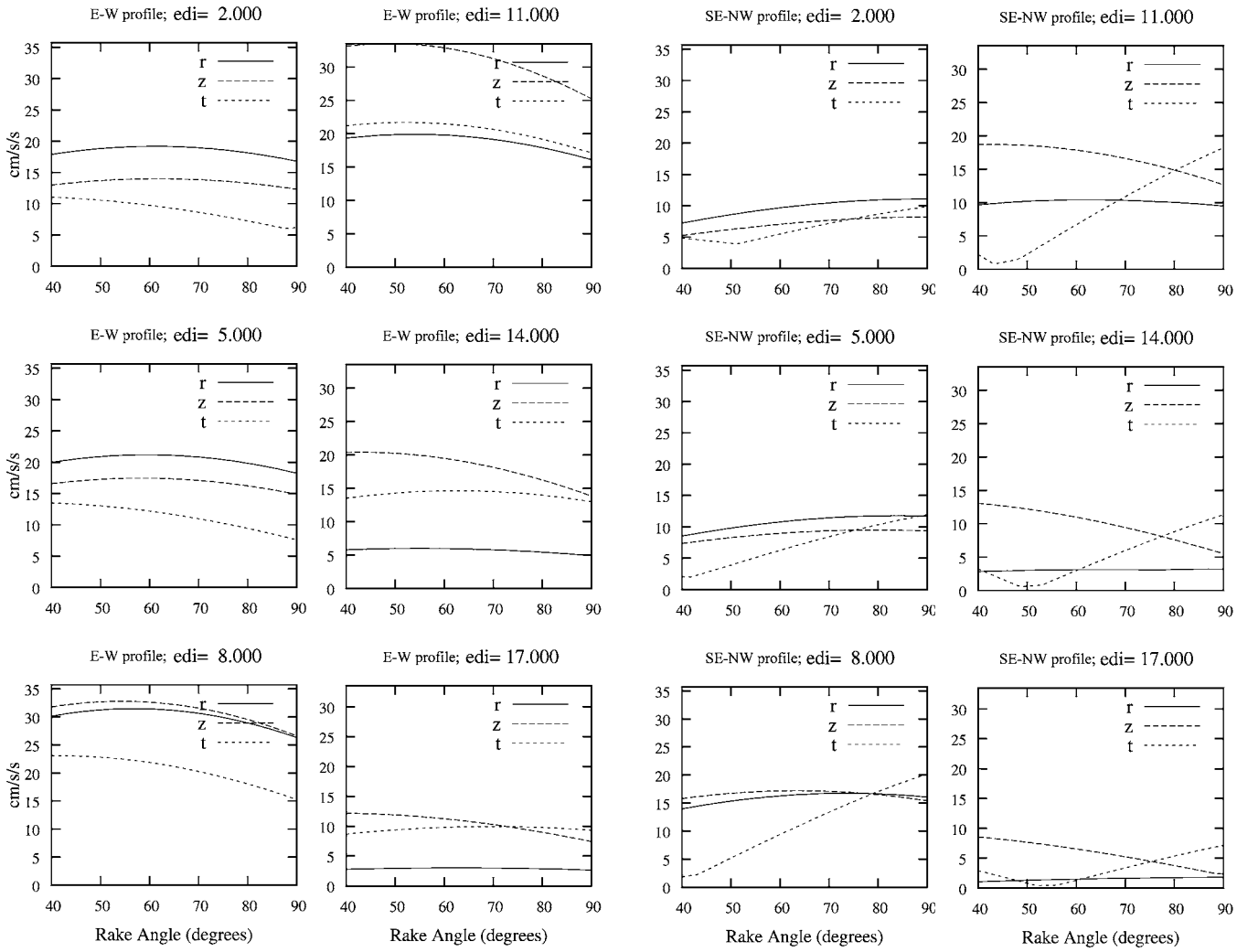

Figure 19. The same as in figure 17 considering the rake angle of the source.

10% around. Site amplification as high as 6 is predicted for the southern part of Tehran, which implies potential for damage. We have shown that if observed data for the studied area are not available, it is possible to simulate the seismic wavefield numerically and thus estimate the site amplification realistically. This is validated by an overall agreement between the synthetic seismograms computed with the hybrid method and the signals recorded during the 2009, $M_w = 4$ Tehran earthquake. A database of synthetic accelerograms represents a scientifically and economically valid tool for seismic microzonation. By more local information on target sites it would be possible to reach a low cost estimation of probable damage and microzonation for cities like Tehran with high potential of seismicity besides highly important political and economical aspects. Defining various scenarios, which can be done as future steps of this study, seems to be necessary for Tehran and similar cities to obtain more realistic information for large earthquakes.

Acknowledgments

We are grateful to the International Centre for Theoretical Physics (ICTP) and International Institute of Earthquake Engineering and Seismology (IIEES) research project number 497-5525, for providing the facilities necessary for this study in the framework of the existing bilateral agreement of cooperation. Parts of the computations have been carried out at the Department of Mathematics and Geosciences of the University of Trieste. Dr Fereidoon Sinaeian of Building and House Research Center of Iran (BHRC) and BHRC itself are highly appreciated for providing strong motion data. Most of the figures are plotted using GMT software (Wessel and Smith 2011). We truly thank two anonymous reviewers for their criticism and comments which helped to improve the manuscript considerably.

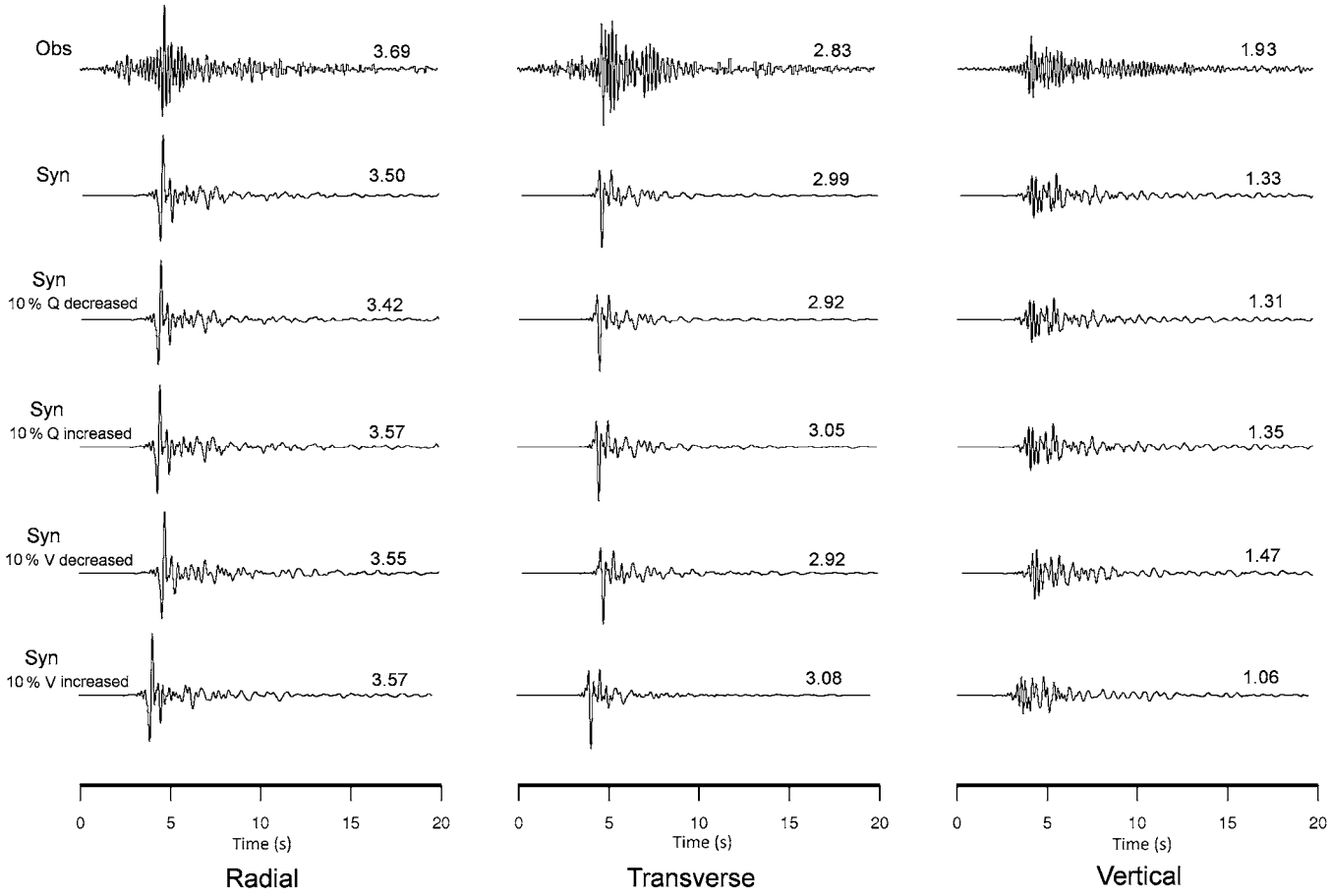

Figure 20. Parametric study on the local structure model which evidences how the model physical properties can change the output synthetic signals. This is a sample of station 5 and the other stations show the same role. All the outputs here are what have been created for station 5 for various changes for three components. It demonstrates the sensitivity of computed ground motion to 10% changes in physical properties of all layers of the sedimentary basin, both increasing and decreasing. Peak values are shown on each signal. Each row is introduced on the left and it is clear that by changing the values 10% the shape of the synthetic seismograms remain rather stable when the amplitudes decrease and increase.

References

Aki K 1987 Strong motion seismology *Strong Ground Motion Seismology (NATO ASI Series, Series C: Mathematical and Physical Sciences* vol 204*)* ed M O Erdik and M Toksoz (Dordrecht: Reidel) pp 3–39

Alford R M, Kelly K R and Boore D M 1974 Accuracy of finite-difference modeling of the acoustic wave equation *Geophysics* **39** 834–42

Ambraseys N N and Melville C P 1982 *A History of Persian Earthquakes* (London: Cambridge University Press) p 219

Dehghani G A and Makris J 1984 The gravity field and crustal structure of Iran *Neues Jahrb Geol. Palaontol. Abh.* **168** 215– 29

Fäh D, Iodice C, Suhadolc P and Panza G F 1993a A new method for the realistic estimation of seismic ground motion in megacities: the case of Rome *Earthq. Spectra* **9** 643–68

Fäh D and Panza G F 1994 Realistic modelling of observed seismic motion in complex sedimentary basins *Ann. Geofis.* **37** 1771–97

Fäh D and Suhadolc P 1995 Application of numerical wave-propagation techniques to study local soil effects: the case of Benevento (Italy) *Pure Appl. Geophys.* **143** 513–36

Fäh D, Suhadolc P, Mueller St and Panza G F 1994 A hybrid method for the estimation of ground motion in sedimentary basin: quantitative modeling for Mexico City *Bull. Seismol. Soc. Am.* **84** 383–99

Fäh D, Suhadolc P and Panza G F 1993b Variability of seismic ground motion in complex media: the Friuli area (Italy) *J. Appl. Geophys.* **30** 131–48

Farahani J and Zare M 2011 The Southeastern Tehran earthquake of 17 October 2009 ($M_w = 4.0$) *Seismol. Res. Lett.* **82** 404–12

Florsch N, Fäh D, Suhadolc P and Panza G F 1991 Complete synthetic seismograms for high-frequency multimode SH-waves *Pageoph* **136** 529–60

Gusev A A 1983 Descriptive statistical model of earthquake source radiation and its application to an estimation of short-period strong motion *Geophys. J. Rev. Astron. Soc.* **74** 787–808

Haghshenas E 2005 Conditions géotechniques et aléa sismique local à Téhéran 2005 *PhD Thesis* Joseph Fourier University (Grenoble I), Grenoble, France

Hamzehloo H, Sinaeian F, Mahood M, Mirzaei Alavijeh H and Farzanegan E 2009 Determination of causative fault parameters *Ray-Tehran Earthquake, Using Near Field SH-Wave Data. JSEE Fall 2009* vol 11 pp 121–31

Hamzehloo H, Vaccari F and Panza G F 2007 Toward a reliable seismic microzonation in Tehran, Iran *Eng. Geol.* **93** 1–16

Japan International Cooperation Agency (JICA) 2000 The study on seismic microzonation of the greater Tehran area in the Islamic republic of Iran *Final Report*

Korn M and Stöckl H 1982 Reflection and transmission of Love channel waves at coal seam discontinuities computed with a finite difference method *J. Geophys.* **50** 171–6

Marrara F and Suhadolc P 1998 Site amplifications in the city of Benevento (Italy): comparison of observed and estimated ground motion from explosive sources *J. Seismol.* **2** 125–43

Nunziata C, Fäh D and Panza G F 1995 Mitigation of seismic hazard of a megacity: the case of Naples *Ann. Geofis.* **38** 649–61

Panza G F 1985 Synthetic seismograms: the Rayleigh waves modal summation *J. Geophys.* **58** 125–45

Panza G F, Romanelli F and Vaccari F 2001 Seismic wave propagation in laterally heterogeneous anelastic media: theory and applications to seismic zonation *Adv. Geophys.* **43** 1–95

Panza G F and Suhadolc P 1987 Complete strong motion synthetics *Seismic Strong Motion Synthetics* ed B A Bolt (Orlando, FL: Academic) pp 153–204

Panza G F, Vaccari F and Romanelli F 1999 The IUGS-UNESCO IGCP Project 414 : realistic modeling of seismic input for megacities and large urban areas *Episodes* **22** 26–32

Rahimi H 2010 Elastic and anelastic regional structures for crust and upper mantle in Iran *PhD Thesis* Int. Inst of Earthquake Engineering and Seismology

Romanelli F, Nunziata C, Natale M and Panza G F 1998a Site response estimation in the Catania area *The Effects of Surface Geology on Seismic Motion* ed K Irikura, K Kudo, H Okada and T Sasatani (Rotterdam: Balkema) pp 1093–100

Romanelli F, Vaccari F and Panza G F 1998b Realistic modelling of ground motion: techniques for site response estimation *Proc. 6th US National Conf. on Earthquake Engineering (Seattle, WA, 31 May–4 June 1998)* CD-ROM: paper 433

Vernant Ph, Nilfroushan F, Chery J, Bayer R, Djamour Y, Masson F, Ritz J F, Sedighi M and Tavakoli F 2004 Deciphering oblique shortening of central Alborz in iran using geodetic data *Earth Planet. Sci. Lett.* **223** 177–85

Virieux J 1986 P-SV wave propagation in heterogeneous media: velocity-stress finite difference method *Geophysics* **51** 889–901

Wessel P and Smith W H F 2011 The generic mapping tools *Technical Reference and Cookbook* Version 4.5.7.

Yaminifard F 2010 Personal Communication, Tehran Disaster Mitigation and Management Organization www.tdmmo.ir